AN ITERATIVE METHOD FOR THE STOKES TYPE PROBLEM WITH VARIABLE VISCOSITY

PIOTR P. GRINEVICH AND MAXIM A. OLSHANSKII*

Abstract. The paper concerns with an iterative technique for solving discretized Stokes type equations with varying viscosity coefficient. We build a special block preconditioner for the discrete system of equations and perform an analysis revealing its properties. The subject of this paper is motivated by numerical solution of incompressible non-Newtonian fluid equations. In particular, the general analysis is applied to the linearized equations of the regularized Bingham model of viscoplastic fluid. Both theoretical analysis and numerical experiments show that the suggested preconditioner leads to a significant improvement of an iterative method convergence compared to a 'standard' preconditioner.

Key words. Iterative methods, saddle-point problem, varying viscosity, non-Newtonian fluid, viscoplastic, Bingham fluid

AMS subject classifications. 65N06, 65N12, 74C10, 76D07

1. Introduction. Certain mathematical models involve flow equations with non-constant viscosity coefficient. This occurs, for example, in geophysical and convection flows, when the viscosity is a function of the temperature, see, e.g., [7, 33], or in turbulent modeling [35]. Another example is non-Newtonian fluids modeling, when the Cauchy stress tensor is given by $\boldsymbol{\sigma} = 2\nu(|\mathbf{Du}|, p)\mathbf{Du} - p\,\mathbf{I}$, where p is the pressure; $\mathbf{Du} = \frac{1}{2}(\nabla\mathbf{u} + \nabla^T\mathbf{u})$ is the rate of the deformation tensor, $\mathbf{u}$ denotes the velocity; $\nu(\cdot)$ is the viscosity which may depend on the second invariant of the rate deformation tensor $|\mathbf{Du}| = \left(\frac{1}{2}\mathrm{tr}([\mathbf{Du}]^2)\right)^{\frac{1}{2}}$ and the pressure. Depending on the specific viscosity function $\nu(\cdot)$ this setting includes the following models (with appropriate parameters ν_0, r, τ_s): Non-newtonian flow due to power law, with $\nu(|\mathbf{Du}|, p) = \nu_0 + \tau_s|\mathbf{Du}|^{r-2}$, e.g. the Bingham model with $r = 1$, non-Newtonian flow with pressure and shear-dependent viscosity, as described for instance in [16, 19] or the Schaeffer model [30, 26] for granular powder flow. Often a regularization is introduced in a model to avoid the singularity of ν for $|\mathbf{Du}| = 0$, see the section 4 for the example of the Bingham regularized model. The Newtonian flow is represented by $\nu(\cdot) = \nu_0$.

In all cases, the velocity $\mathbf{u}$ and the pressure p satisfy the following generalized Navier-Stokes equations

$$\frac{\partial \mathbf{u}}{\partial t} + \mathbf{u}\cdot\nabla\mathbf{u} - \mathbf{div}\nu(|\mathbf{Du}|, p)\mathbf{Du} + \nabla p = \mathbf{g}, \quad \mathrm{div}\ \mathbf{u} = \mathbf{0}\,. \tag{1.1}$$

We assume that equations (1.1) hold in the whole computational domain $\Omega \subset \mathbb{R}^d$, $d = 2, 3$. This may require a regularization for the case of $\nu \to \infty$. Further we consider a steady flow and neglect the inertia terms. In remark 4 we discuss how the results of the paper can be extended for the case unsteady flows and if the inertia terms are taken into account. The resulting system of equations can be written in the form:

$$F(\mathbf{u}, p) \circ \begin{pmatrix} \mathbf{u} \\ p \end{pmatrix} = \begin{pmatrix} \mathbf{g} \\ 0 \end{pmatrix}, \qquad \mathbf{u} = \mathbf{u}_b \ \text{ on } \ \partial\Omega \tag{1.2}$$

* Department of Mechanics and Mathematics, Moscow State M.V. Lomonosov University, Moscow 119899, Russia; email: Maxim.Olshanskii(at)mtu-net.ru. This work was supported by the German Research Foundation and the Russian Foundation for Basic Research through projects 08-01-91957 and 08-01-00159

with the *linear* operator (for a fixed vector function $\mathbf{a}$ and scalar function ξ) of the following 2×2 block form

$$F(\mathbf{a}, \xi) := \begin{pmatrix} -\mathbf{div}\, \nu(|\mathbf{D}\mathbf{a}|, \xi)\mathbf{D} & \nabla \\ -\mathrm{div} & 0 \end{pmatrix} \tag{1.3}$$

For simplicity we assumed the Dirichlet boundary conditions in (1.2) with some $\mathbf{u}_b$ prescribed on the boundary of Ω, such that $\int_{\partial\Omega} \mathbf{u}_b \cdot \mathbf{n} = 0$. We solve (1.2) with the Picard type iterative method:

$$\begin{pmatrix} \mathbf{u}^n \\ p^n \end{pmatrix} = \begin{pmatrix} \mathbf{u}^{n-1} \\ p^{n-1} \end{pmatrix} - \widetilde{F}(\mathbf{u}^{n-1}, p^{n-1})^{-1} \circ \left[F(\mathbf{u}^{n-1}, p^{n-1}) \circ \begin{pmatrix} \mathbf{u}^{n-1} \\ p^{n-1} \end{pmatrix} - \begin{pmatrix} \mathbf{g} \\ 0 \end{pmatrix} \right]. \tag{1.4}$$

Here $\widetilde{F}(\mathbf{u}^{n-1}, p^{n-1})^{-1}$ is an *approximate* solution to the linear problem

$$F(\mathbf{u}^{n-1}, p^{n-1}) \circ \begin{pmatrix} \mathbf{v} \\ q \end{pmatrix} = \begin{pmatrix} \mathbf{f} \\ g \end{pmatrix}, \qquad \mathbf{v} = 0 \ \text{ on } \ \partial\Omega, \tag{1.5}$$

with $\mathbf{f}$ and g standing for corresponding residuals from (1.4) in momentum and continuity equations, respectively. Given $\mathbf{u}^{n-1}$ and p^{n-1} the problem (1.5) can bewritten as the Stokes type problem with the variable viscosity coefficient $\nu(\mathbf{x})$:

$$\begin{aligned} -\mathbf{div}\nu(\mathbf{x})\mathbf{D}\mathbf{v} + \nabla q = \mathbf{f} \quad &\text{on} \quad \Omega, \\ -\mathrm{div}\ \mathbf{v} = g \quad &\text{on} \quad \Omega, \\ \mathbf{v} = 0 \quad &\text{on} \quad \partial\Omega. \end{aligned} \tag{1.6}$$

Obviously, solving (1.6) is the most computationally consuming step in the entire approach. Of course, in practice (1.4) is applied to the system of *discretized* equations. Thus the main concern of the paper is the development and analysis of preconditioned iterative methods for solving the discrete counterpart of (1.6).

The rest of the paper is organized as follows. In section 2 we consider a general iterative approach for solving (1.6) and in section 3 we discuss and analyze some choices of preconditioners. In section 4 the analysis is applied to the particular case of the regularized Bingham model of non-Newtonian fluid. Section 5 collects the results of numerical experiments for two model problems of the Bingham fluid flows discretized with finite element and finite difference methods.

2. Linear solver. In this section we deal with a discrete counterpart of (1.6). Here and in the remainder the L^2 scalar product and associated norm are denoted by $(\cdot, \cdot)$ and $\|\cdot\|$, respectively. Moreover, we will simply use the notation ν for the variable viscosity coefficient. To define the pressure space uniquely some factorization of $L^2(\Omega)$ is introduced. In this paper we will use two different factorizations:

$$L^2_0(\Omega) := \{q \in L^2(\Omega) : (q, 1) = 0\} \quad \text{and} \quad L^2_\nu(\Omega) := \{q \in L^2(\Omega) : (q, \nu^{-1}) = 0\}.$$

To fix an idea let us consider finite element velocity $\mathbb{V}_h \subset \mathbf{H}^1_0(\Omega)$ and pressure $\mathbb{Q}_h \subset L^2_0(\Omega)$ spaces. Assume that the pair of spaces $\mathbb{V}_h$, $\mathbb{Q}_h$ is stable in the LBB sense (see, e.g., [2]), i.e. there exists a mesh independent constant $c_0 > 0$ such that

$$c_0 \le \inf_{q_h \in \mathbb{Q}_h} \sup_{\mathbf{v}_h \in \mathbb{V}_h} \frac{(q_h, \mathrm{div}\, \mathbf{v}_h)}{\|q_h\| \, \|\nabla \mathbf{v}_h\|}. \tag{2.1}$$

Here and in the remainder we always take $\inf_x$ or $\sup_x$ over nonzero elements if $\|x\|$ appears in the denominator. The finite element discretization of (1.6) consists in finding $\mathbf{u}_h \in \mathbb{V}_h$ and $p_h \in \mathbb{Q}_h$ such that

$$(\nu \mathbf{D}\mathbf{u}_h, \mathbf{D}\mathbf{v}_h) - (p_h, \operatorname{div} \mathbf{v}_h) + (q_h, \operatorname{div} \mathbf{u}_h) = (\mathbf{f}_h, \mathbf{v}_h) - (g_h, q_h) \quad \forall\, \mathbf{v}_h \in \mathbb{V}_h,\ q_h \in \mathbb{Q}_h. \tag{2.2}$$

Let $\{\phi_i\}_{1\le i\le n}$ and $\{\psi_j\}_{1\le j\le m}$ be nodal basis of $\mathbb{V}_h$ and $\mathbb{Q}_h$, respectively. Define the following matrices: $A = \{A_{i,j}\} \in \mathbb{R}^{n\times n}$, $B = \{B_{i,j}\} \in \mathbb{R}^{m\times n}$ and $M = \{M_{i,j}\} \in \mathbb{R}^{m\times m}$ with

$$A_{i,j} = (\nu \mathbf{D}\phi_j, \mathbf{D}\phi_i), \quad B_{i,j} = -(\operatorname{div} \phi_j, \psi_i), \quad M_{i,j} = (\psi_j, \psi_i).$$

The linear algebraic system corresponding to (2.2) takes the form:

$$\begin{pmatrix} A & B^T \\ B & 0 \end{pmatrix} \begin{pmatrix} u \\ p \end{pmatrix} = \begin{pmatrix} f \\ g \end{pmatrix}. \tag{2.3}$$

We are interested in solving (2.3) by a preconditioned iterative method. Following the approach from [31], we consider the block diagonal preconditioner for the system (2.3):

$$\mathcal{P} = \begin{pmatrix} \widehat{A} & 0 \\ 0 & -\widehat{S} \end{pmatrix}. \tag{2.4}$$

The matrix $\widehat{A}$ is a preconditioner for the matrix A, such that $\widehat{A}^{-1}$ may be considered as an inexact solver for linear systems involving A. The matrix $\widehat{S}$ is a preconditioner for the pressure Schur complement of (2.3) $S = BA^{-1}B^T$. In an iterative algorithm one needs the actions of $\widehat{A}^{-1}$ and $\widehat{S}^{-1}$ on subvectors, rather than the matrices $\widehat{A}$, $\widehat{S}$ explicitly. Once good preconditioners for A and S are given, an appropriate Krylov subspace iterative method for (2.3) such as MINRES [29] with the block preconditioner (2.4) is an efficient solver.

Given preconditioners $\widehat{A}^{-1}$ and $\widehat{S}^{-1}$ one has the choice of several other iterative techniques for solving the problem (2.3). It includes a preconditioned conjugate gradient method through a special transformation of (2.3) [5] and inexact Uzawa type method [1], see also the review paper [3]. As an option we also use the approach well suited for more general nonsymmetric problems (see remark 4) of the same structure [12]: The BiCGstab iterative method with the block triangular preconditioner:

$$\mathcal{P}_1 = \begin{pmatrix} \widehat{A} & 0 \\ B & -\widehat{S} \end{pmatrix}. \tag{2.5}$$

In the literature one can find geometric or algebraic multigrid (see, e.g. [15, 32, 22]) or domain decomposition [28] iterative algorithms which provide effective preconditioners $\widehat{A}$ if the function ν is sufficiently regular, see remark 3, however. At the same time, building a preconditioner for S is a more delicate issue, since S is given *implicitly* and S is *not* a sparse matrix. In the next section we analyze two preconditioners for S.

3. Schur complement preconditioning. The matrix S has one dimensional kernel, corresponding to the constant pressure mode. Further we will consider S as an operator on an appropriate subspace[1]. Thus, when it does not cause a confusion

[1] This $m-1$ dimensional subspace can be characterized as all $q \in \mathbb{R}^m$ such that $q_h \in \mathbb{Q}_h$, where q is the vector of (nodal) coefficients for q_h.

we treat S as a nonsingular matrix. For the Stokes problem it is well known that S is spectrally equivalent to the pressure mass matrix M. The lemma 3.1 below extends the result to the case of variable viscosity coefficient and the rate of deformation tensor formulation. For two matrices A and B we write $A \geq B$ iff $A - B$ is semi-positive definite. We will use the notation $\langle \cdot, \cdot \rangle$ for the Euclidean scalar product.
Denote

$$\nu_{\min} = \inf_{\Omega} \nu(\mathbf{x}), \qquad \nu_{\max} = \sup_{\Omega} \nu(\mathbf{x}).$$

The natural assumption is that $\nu_{\min} > 0$ and $\nu_{\max} < \infty$.

LEMMA 3.1. *Assume* (2.1), *then it holds*

$$c_0^2 \nu_{\max}^{-1} M \leq S \leq \nu_{\min}^{-1} M. \tag{3.1}$$

Proof. For arbitrary pressure finite element function $q_h \in \mathbb{Q}_h$ denote by q the corresponding vector of coefficients from $\mathbb{R}^m$. Due to definitions of matrices A, B and M it holds

$$\langle S\, q, q \rangle = \langle A^{-1} B^T\, q, B^T\, q \rangle = \sup_{v \in \mathbb{R}^n} \frac{\langle v, B^T\, q \rangle^2}{\langle A\, v, v \rangle} = \sup_{\mathbf{v}_h \in \mathbb{V}_h} \frac{(q_h, \operatorname{div} \mathbf{v}_h)^2}{\|\nu^{\frac{1}{2}} \mathbf{D} \mathbf{v}_h\|^2}, \tag{3.2}$$

$$\langle M\, q, q \rangle = \|q_h\|^2. \tag{3.3}$$

Note that due to the identities $\operatorname{rot}^2 + \nabla \operatorname{div} = \Delta = 2\mathbf{div}\mathbf{D} - \nabla \operatorname{div}$ it holds (one can apply integration by parts to verify)

$$\|\operatorname{rot} \mathbf{v}\|^2 + \|\operatorname{div} \mathbf{v}\|^2 = \|\nabla \mathbf{v}\|^2 = 2\|\mathbf{D}\mathbf{v}\|^2 - \|\operatorname{div} \mathbf{v}\|^2 \qquad \forall\ \mathbf{v} \in \mathbf{H}_0^1(\Omega).$$

Hence

$$\|\operatorname{div} \mathbf{v}\|^2 \leq \|\mathbf{D}\mathbf{v}\|^2 \leq \|\nabla \mathbf{v}\|^2 \qquad \forall\ \mathbf{v} \in \mathbf{H}_0^1(\Omega). \tag{3.4}$$

Using estimates (3.4), embedding $\mathbb{V}_h \subset \mathbf{H}_0^1(\Omega)$ and the Cauchy inequality we get

$$\|\nu^{\frac{1}{2}} \mathbf{D} \mathbf{v}_h\|^2 \leq \nu_{\max} \|\mathbf{D}\mathbf{v}_h\|^2 \leq \nu_{\max} \|\nabla \mathbf{v}_h\|^2. \tag{3.5}$$

and

$$(q_h, \operatorname{div} \mathbf{v}_h) \leq \|q_h\| \|\operatorname{div} \mathbf{v}_h\| \leq \|q_h\| \|\mathbf{D}\mathbf{v}_h\| \leq \nu_{\min}^{-\frac{1}{2}} \|q_h\| \|\nu^{\frac{1}{2}} \mathbf{D} \mathbf{v}_h\|. \tag{3.6}$$

Relations (3.2), (3.3) together with estimates (3.5)–(3.6) and (2.1) yield

$$c_0^2 \nu_{\max}^{-1} \langle M\, q, q \rangle \leq \langle S\, q, q \rangle \leq \nu_{\min}^{-1} \langle M\, q, q \rangle.$$

Thus the lemma is proved
□

From the result of the lemma it follows

$$\operatorname{cond}(\widehat{S}^{-1} S) \leq c_0^{-2} \frac{\nu_{\max}}{\nu_{\min}} \qquad \text{with } \ \widehat{S} = M. \tag{3.7}$$

Since M^{-1} is not a sparse matrix, it is a common approach to use instead of M a diagonal approximation $\widehat{M} = \operatorname{diag}(M)$ as a preconditioner for S. For a family of

grids satisfying minimal angle condition it holds [37] $c_m\widehat{M} \le M \le C_m\widehat{M}$ with positive mesh-independent constants c_m and C_m. Therefore, an estimate similar to (3.7) holds with M replaced by $\widehat{M}$. In either case the resulting preconditioner becomes inefficient for problems with the large ratio $\nu_{\max}/\nu_{\min}$. Since in particular application of our interest it often holds $\nu_{\max}/\nu_{\min} \gg 1$, we suggest a new preconditioner below, which accounts for the variable coefficient ν. To this end, define the following mass type matrix $M_\nu = \{(M_\nu)_{i,j}\} \in \mathbb{R}^{m\times m}$ with

$$(M_\nu)_{i,j} = (\nu^{-1}\psi_j, \psi_i). \tag{3.8}$$

In the remainder of this section we assume $\mathbb{Q}_h \subset L^2_\nu$. In [24] it was proved that for the case of *piecewise constant* $\nu(\mathbf{x}) = \begin{cases} \nu_1, & \mathbf{x} \in \Omega_1 \\ \nu_2, & \mathbf{x} \in \Omega \setminus \Omega_1 \end{cases}$ the inequalities

$$c_\nu M_\nu \le S \le C_\nu M_\nu \tag{3.9}$$

hold with constants $c_\nu > 0$ and C_ν independent of mesh size and the values of $\nu_1 > 0$ and $\nu_2 > 0$ (c_ν and C_ν depend, however, on Ω_1). This observation as well as the simple scaling argument: $S \to \lambda^{-1}S$ if $\nu \to \lambda\nu$, lead us to the choice of M_ν as a preconditioner to S. One can easily prove the following result.

LEMMA 3.2. *For a positive $\nu \in L^\infty(\Omega)$ and $\Omega \subset \mathbb{R}^d$ the upper bound in* (3.9) *holds with $C_\nu = d$.*

Proof. By direct computation we verify the inequality $\|\nu^{\frac12}\operatorname{div}\mathbf{v}\| \le \sqrt{d}\|\nu^{\frac12}\mathbf{D}\mathbf{v}\|$ for any $\mathbf{v} \in \mathbf{H}^1_0(\Omega)$. This and the Cauchy inequality give

$$\sup_{\mathbf{v}_h\in\mathbb{V}_h} \frac{(q_h, \operatorname{div}\mathbf{v}_h)^2}{\|\nu^{\frac12}\mathbf{D}\mathbf{v}_h\|^2} \le \sup_{\mathbf{v}_h\in\mathbb{V}_h} \frac{\|\nu^{-\frac12}q_h\|^2\|\nu^{\frac12}\operatorname{div}\mathbf{v}_h\|^2}{\|\nu^{\frac12}\mathbf{D}\mathbf{v}_h\|^2} \le d\|\nu^{-\frac12}q_h\|^2 = d\langle M_\nu\, q, q\rangle \tag{3.10}$$

for any $q_h \in \mathbb{Q}_h$ and the corresponding vector of coefficients q. Now results in (3.2) and (3.10) prove the lemma. □

Using arguments similar to the proof of lemma 3.1, it is easy to show that the constant c_ν in (3.9) can be taken as $c_\nu = c_0^2\nu_{\min}\nu_{\max}^{-1}$. In many cases this would be a far not optimal bound; it does not give any improvement of the estimate of $\operatorname{cond}(\widehat{S}^{-1}S)$ compared to (3.7). Numerical experiments show that for particular ν-s appearing in non-Newtonian flow calculations the (effective) condition number of $M_\nu^{-1}S$ is uniformly bounded with respect to $\nu_{\min}\nu_{\max}^{-1}$, while the result in (3.7) is sharp. To gain a better insight and to prove a tighter low bound in (3.9) we consider the 'continuous' setting of the problem, i.e. instead of finite element spaces and operators we consider the original differential ones. In such a setting the low bound in (3.9) is equivalent to the following estimate (cf. (3.2),(3.8)) for any $q \in L^2_\nu(\Omega)$:

$$\tilde{c}_\nu\|\nu^{-\frac12}q\|^2 \le \sup_{\mathbf{v}\in\mathbf{H}^1_0(\Omega)} \frac{(q, \operatorname{div}\mathbf{v})^2}{\|\nu^{\frac12}\mathbf{D}\mathbf{v}\|^2}. \tag{3.11}$$

with $\tilde{c}_\nu > 0$. Note that for $\nu \equiv 1$ (3.11) is equivalent to the *Nečas inequality* (the continuous counterpart of the LBB condition (2.1)).

First we prove the following lemma.

LEMMA 3.3. *Assume that ν is sufficiently smooth, so the norms below make sense. Then* (3.11) *holds for any $q \in L^2_\nu(\Omega)$ such that $(q, \nu^{-\frac12}) = 0$ with the constant $\tilde{c}_\nu$ defined below. If $d = 2$, then*

$$\tilde{c}_\nu = \tilde{c}_0(1 + c(k,s)\,\|\nu^{\frac12}\|_{L^k}\|\nabla\nu^{-\frac12}\|_{L^{r+s}})^{-2} \tag{3.12}$$

with any $k > 2$, $s > 0$, and $r = \frac{2k}{k-2}$. Here $c(k,s)$ depends on constants from embedding inequalities of $H^1_0(\Omega)$ into $L^t(\Omega)$ with $t = t(s,k)$, and $\tilde{c}_0$ depends only on the constant from the Nečas inequality. If $d = 3$, then

$$\tilde{c}_\nu = \tilde{c}_0(1 + c\,\|\nu^{\frac{1}{2}}\|_{L^k}\|\nabla\nu^{-\frac{1}{2}}\|_{L^r})^{-2} \tag{3.13}$$

with any $k > 3$ and $r = \frac{3k}{k-3}$.

Proof. The Nečas inequality is equivalent to the following result: For any $r \in L^2_0(\Omega)$ there exists $\mathbf{w} \in \mathbf{H}^1_0(\Omega)$ such that

$$\operatorname{div}\mathbf{w} = r \qquad \text{and} \qquad \|\nabla\mathbf{w}\| \le C\,\|r\| \tag{3.14}$$

with a constant C depending only on Ω. For an arbitrary $q \in L^2_\nu(\Omega)$ satisfying $(q, \nu^{-\frac{1}{2}}) = 0$ consider $\mathbf{w}$ given by (3.14) for $r = \nu^{-\frac{1}{2}}q \in L^2_0(\Omega)$. Observe the identity

$$\operatorname{div}(\nu^{-\frac{1}{2}}\mathbf{w}) = \nu^{-\frac{1}{2}}\operatorname{div}\mathbf{w} + \mathbf{w}\cdot\nabla\nu^{-\frac{1}{2}}. \tag{3.15}$$

Note that $(\nu^{-\frac{1}{2}}\operatorname{div}\mathbf{w}, 1) = (\nu^{-1}q, 1) = 0$ and $(\operatorname{div}(\nu^{-\frac{1}{2}}\mathbf{w}), 1) = (\nu^{-\frac{1}{2}}\mathbf{w}, \nabla 1) = 0$, due to (3.15) this yields $(\mathbf{w}\cdot\nabla\nu^{-\frac{1}{2}}, 1) = 0$. Therefore, we may define $\mathbf{u} \in \mathbf{H}^1_0(\Omega)$ solving the following Stokes problem

$$\begin{aligned} -\Delta\mathbf{u} + \nabla\xi = 0, \quad \operatorname{div}\mathbf{u} = \mathbf{w}\cdot\nabla\nu^{-\frac{1}{2}} \quad &\text{on} \quad \Omega \\ \mathbf{u} = 0 \quad &\text{on} \quad \partial\Omega \end{aligned}$$

One has the following *a priori* estimate for the solution of the Stokes problem [34]:

$$\|\nabla\mathbf{u}\|_{L^s} \le C\,\|\mathbf{w}\cdot\nabla\nu^{-\frac{1}{2}}\|_{L^s} \qquad \forall\ s > 1. \tag{3.16}$$

Now we set $\mathbf{v} = \nu^{-\frac{1}{2}}\mathbf{w} - \mathbf{u}$. Thanks to (3.14) and (3.15), it holds

$$(\operatorname{div}\mathbf{v}, q) = (\operatorname{div}\mathbf{w}, \nu^{-\frac{1}{2}}q) = \|\nu^{-\frac{1}{2}}q\|^2. \tag{3.17}$$

It remains to estimate $\|\nu^{\frac{1}{2}}\mathbf{D}\mathbf{v}\|$. We have

$$\|\nu^{\frac{1}{2}}\mathbf{D}\mathbf{v}\| \le c\|\nu^{\frac{1}{2}}\nabla\mathbf{v}\| \le c(\|\nu^{\frac{1}{2}}\nabla(\nu^{-\frac{1}{2}}\mathbf{w})\| + \|\nu^{\frac{1}{2}}\nabla\mathbf{u}\|). \tag{3.18}$$

We assume now $d = 2$ and estimate the terms on the right hand side of (3.18) separately. Using Holder's inequality and the embedding inequality $\|\mathbf{w}\|_{L^r} \le c(r)\|\nabla\mathbf{w}\|$, $\forall r \in [1,\infty)$, we get

$$\begin{aligned} \|\nu^{\frac{1}{2}}\nabla(\nu^{-\frac{1}{2}}\mathbf{w})\| &\le \|\nabla\mathbf{w}\| + \|\nu^{\frac{1}{2}}\mathbf{w}\cdot\nabla\nu^{-\frac{1}{2}}\| \\ &\le \|\nabla\mathbf{w}\| + \|\nu^{\frac{1}{2}}\nabla\nu^{-\frac{1}{2}}\|_{L^{2k}}\|\mathbf{w}\|_{L^{2r}} \quad (r = \tfrac{k}{k-1}) \\ &\le (1 + c(k)\|\nu^{\frac{1}{2}}\nabla\nu^{-\frac{1}{2}}\|_{L^{2k}})\|\nabla\mathbf{w}\| \qquad \forall\ k > 1. \end{aligned} \tag{3.19}$$

Using Holder's inequality, embedding inequalities and (3.16), we estimate the second term

$$\begin{aligned} \|\nu^{\frac{1}{2}}\nabla\mathbf{u}\| &\le \|\nu^{\frac{1}{2}}\|_{L^{2k}}\|\nabla\mathbf{u}\|_{L^{2r}} \le c\,\|\nu^{\frac{1}{2}}\|_{L^{2k}}\|\mathbf{w}\cdot\nabla\nu^{-\frac{1}{2}}\|_{L^{2r}} \\ &\le c(s)\,\|\nu^{\frac{1}{2}}\|_{L^{2k}}\|\nabla\nu^{-\frac{1}{2}}\|_{L^{2r+s}}\|\nabla\mathbf{w}\| \qquad \forall\ k > 1,\ s > 0,\ r = \tfrac{k}{k-1} \end{aligned} \tag{3.20}$$

Note that Holder's inequality gives $\|\nu^{\frac{1}{2}}\nabla\nu^{-\frac{1}{2}}\|_{L^{2k}} \le \|\nu^{\frac{1}{2}}\|_{L^{\ell}}\|\nabla\nu^{-\frac{1}{2}}\|_{L^{2k\ell/(\ell-2k)}}$ for any $\ell > 2$. We take k sufficiently close to 1, so to ensure $2k\ell/(\ell-2k) \le 2\ell/(\ell-2)$. Therefore, from (3.18)–(3.20) and (3.14) with $r = \nu^{-\frac{1}{2}}q$ we obtain

$$\|\nu^{\frac{1}{2}}\mathbf{D}\mathbf{v}\| \le c\,(1 + c(s)\,\|\nu^{\frac{1}{2}}\|_{L^{\ell}}\|\nabla\nu^{-\frac{1}{2}}\|_{L^{r+s}})\|\nu^{-\frac{1}{2}}q\|. \tag{3.21}$$

with any $\ell > 2$, $s > 0$, and $r = \frac{2\ell}{\ell-2}$. Relations (3.17) and (3.21) yield (3.11) with $\tilde{c}_\nu$ as in (3.12).

We assume now $d = 3$. In this case it holds $\|\mathbf{w}\|_{L^6} \le c\,\|\nabla\mathbf{w}\|$. With the same arguments as in (3.19)–(3.21) we get

$$\|\nu^{\frac{1}{2}}\nabla(\nu^{-\frac{1}{2}}\mathbf{w})\| \le (1 + c\,\|\nu^{\frac{1}{2}}\nabla\nu^{-\frac{1}{2}}\|_{L^3})\|\nabla\mathbf{w}\| \tag{3.22}$$

and

$$\|\nu^{\frac{1}{2}}\nabla\mathbf{u}\| \le c\,\|\nu^{\frac{1}{2}}\|_{L^{2k}}\|\nabla\nu^{-\frac{1}{2}}\|_{L^{2r}}\|\nabla\mathbf{w}\| \qquad \forall\ k \ge \tfrac{3}{2},\ r = \tfrac{3k}{2k-3}. \tag{3.23}$$

Holder's inequality gives $\|\nu^{\frac{1}{2}}\nabla\nu^{-\frac{1}{2}}\|_{L^3} \le \|\nu^{\frac{1}{2}}\|_{L^{3k}}\|\nabla\nu^{-\frac{1}{2}}\|_{L^{3k/(k-1)}}$. Therefore, it holds

$$\|\nu^{\frac{1}{2}}\mathbf{D}\mathbf{v}\| \le c\,(1 + c\,\|\nu^{\frac{1}{2}}\|_{L^{k}}\|\nabla\nu^{-\frac{1}{2}}\|_{L^{r}})\|\nu^{-\frac{1}{2}}q\|. \tag{3.24}$$

with any $k > 3$ and $r = \frac{3k}{k-3}$. Relations (3.17) and (3.24) yield (3.11) with $\tilde{c}_\nu$ as in (3.13).
□

Estimates (3.12) and (3.13) can be more useful than the trivial one ($c_\nu = c_0^2\nu_{\min}\nu_{\max}^{-1}$) since they involve integral norms of ν. However, from the example of the Bingham fluid we will see that one may encounter situations when ν is only piecewise smooth and $\nu = \nu_{\max}$ in a subdomain $\Omega_1 \subset \Omega$ with $\mathrm{meas}(\Omega_1) > 0$. By a domain decomposition argument the result of lemma 3.3 can be improved to provide useful bounds of $\tilde{c}_\nu$ in this case. Thus, we prove the following lemma.

LEMMA 3.4. *Let $\overline{\Omega} = \cup_{i=1}^{N}\overline{\Omega}_i$, where Ω_i are connected subdomains with sufficiently regular boundary. Assume that ν is piecewise smooth with respect to this partitioning. Then* (3.11) *holds for any $q \in L^2(\Omega)$ such that $(q, \nu^{-\frac{1}{2}})_{L_2(\Omega_i)} = (q, \nu^{-1})_{L_2(\Omega_i)} = 0$ with $\tilde{c}_\nu = \min\limits_{1\le i\le N}\tilde{c}_\nu(\Omega_i)$, where $\tilde{c}_\nu(\Omega_i)$ is the constant given by* (3.12) *or* (3.13) *for the domain Ω_i.*

Proof. Due to lemma 3.3 in each Ω_i we can define $\mathbf{v}_i \in \mathbf{H}_0^1(\Omega_i)$ such that

$$(\mathrm{div}\,\mathbf{v}_i, q)_{L^2(\Omega_i)} = \|\nu^{-\frac{1}{2}}q\|^2_{L^2(\Omega_i)}, \qquad \tilde{c}_\nu(\Omega_i)^{\frac{1}{2}}\|\nu^{\frac{1}{2}}\mathbf{D}\mathbf{v}_i\|_{L^2(\Omega_i)} \le \|\nu^{-\frac{1}{2}}q\|_{L^2(\Omega_i)}.$$

For all i we extend $\mathbf{v}_i$ by zero to the whole domain Ω and set $\mathbf{v} = \sum_{i=1}^{N}\mathbf{v}_i$. We get

$$(\mathrm{div}\,\mathbf{v}, q) = \|\nu^{-\frac{1}{2}}q\|^2, \qquad \min_{1\le i\le N}\tilde{c}_\nu(\Omega_i)^{\frac{1}{2}}\,\|\nu^{\frac{1}{2}}\mathbf{D}\mathbf{v}\| \le \|\nu^{-\frac{1}{2}}q\|.$$

□

REMARK 1. Consider the eigenvalue problem

$$Sx = \lambda M_\nu x. \tag{3.25}$$

The corresponding eigenvalues λ are real and the Courant–Fischer Theorem gives for the k-th eigenvalue the characterization

$$\lambda_k = \max_{\mathcal{K}\in\mathcal{V}_{k-1}} \min_{x\in\mathcal{K}^\perp} \frac{\langle Sx, x\rangle}{\langle M_\nu x, x\rangle}\,, \tag{3.26}$$

where $\mathcal{V}_{k-1}$ denotes the family of all $(k-1)$-dimensional subspaces of $\mathbb{R}^m$. If we *assume* that discrete counterparts of the estimate (3.11) and lemma 3.4 are valid, then (3.26) immediately gives the following result. The eigenvalues of (3.25) satisfy

$$0 = \lambda_1 < \lambda_2 \le \lambda_3 \le \cdots \le \lambda_m \le d \quad \text{and} \quad \tilde{c}_\nu \le \lambda_{2N+1} \tag{3.27}$$

with $d = 2$ or $d = 3$.

Note that $2N-1$ small eigenvalues would add at most $2N-1$ extra iterations of a preconditioned Krylov subspace method like MINRES to converge with desired tolerance. Therefore, if the number of subdomains N is small (this is the case in applications considered further), then the convergence rate is essentially determined by the value $\tilde{c}_\nu$. We also recall that the iterative method does not account for $\lambda_1 = 0$, since the pressure approximations always belong to the proper subspace.

Remark 2. In iterative process (1.4) one may also define $\widetilde{F}(\mathbf{u}^{n-1}, p^{n-1})^{-1}$ as an approximate inverse of the Jacobian of the system. This would lead to an inexact Newton method for (1.2). Although this approach leads potentially to quadratically convergent iterations, one has to choose a sufficiently good initial guess. Moreover, the linear system on each iteration looses the symmetric structure as in (2.3) and the (1,1)-block A is not necessarily positive definite any more. The latter may lead to the further loss of linear algebraic solvers efficiency. However, this inexact Newton approach is of potential interest and will be considered in a forthcoming paper.

Remark 3. Standard analysis of optimal solvers such as multigrid methods for discrete diffusion equation relies on bounds for the minima and some norms of the diffusion coefficient. Since such uniform bounds do not necessarily hold for $\nu(\mathbf{x})$, the application of these methods for solving or preconditioning the submatrix A should be done with some care. To separate the effect of preconditioning the submatrix A from the effect of preconditioning the Schur complement matrix S we use the exact factorization of A in our numerical experiments. The analysis of optimal preconditioning strategies for A in conjunction with non-Newtonian fluid modeling is not a subject of this paper.

Remark 4. If the inertia terms are included in the model of non-Newtonian flow, they can be treated by an algebraic solver in several ways. One option is to treat them explicitly and include only in the residual part of (1.2). This would lead to the same linearized problem as before on every non-linear iteration. Alternatively, one may linearize the inertia terms and include them in the definition of $\widetilde{F}(\mathbf{u}^{n-1}, p^{n-1})^{-1}$. In this case (2.3) would correspond to the Oseen type problem with variable viscosity. One may combine the techniques discussed in [12, 25] with the results of the present paper. The time-dependent case does not cause any additional difficulties. In general, it typically leads to a better conditioned matrix A and the pressure Schur complement preconditioner $\widehat{S}^{-1}$ should include an approximate pressure Poisson solve, cf. [6, 18].

4. Application to the Bingham problem. Here we apply the analysis of the previous section to the regularized Bingham model of viscoplastic fluid. We will show that for a particular flow, when the norms of ν can be evaluated explicitly, the estimate of lemma 3.4 provides a useful bound on the eigenvalues of the preconditioned

operator. In the next section the effect of different preconditioning will be illustrated numerically.

Let $\Omega \in \mathbb{R}^d$, $d = 2, 3$, be a bounded connected domain. A slow and steady flow of the viscoplastic Bingham fluid is described by the following system of equations

$$\begin{aligned} -\mathbf{div}\,\boldsymbol{\tau} + \nabla p &= \mathbf{f}, \\ \operatorname{div}\mathbf{u} &= 0, \\ \mathbf{u} &= \mathbf{u}_b \quad \text{on} \quad \partial\Omega \end{aligned} \tag{4.1}$$

and constitutive relations

$$\begin{aligned} \boldsymbol{\tau} = 2\mu\mathbf{D}\mathbf{u} + \tau_s \frac{\mathbf{D}\mathbf{u}}{|\mathbf{D}\mathbf{u}|}, \quad &\text{if} \quad |\mathbf{D}\mathbf{u}| \neq 0, \\ |\boldsymbol{\tau}| \leq \tau_s, \quad &\text{if} \quad |\mathbf{D}\mathbf{u}| = 0, \end{aligned} \tag{4.2}$$

where $\mathbf{u}, p, \boldsymbol{\tau}$ are unknown velocity, pressure and stress tensor, μ is a constant plastic viscosity, τ_s is the yield stress. For $\tau_s = 0$ the system (4.1)–(4.2) reduces to the Stokes problem.

If $\tau_s > 0$ the equations (4.1) are imposed only in the *flow region*, where $|\mathbf{D}\mathbf{u}| > 0$, and make no sense in the *rigid region* $\Omega_r = \{\mathbf{x} \in \Omega \,|\, \mathbf{D}\mathbf{u}(\mathbf{x}) = 0\}$. Both regions are *a priori* unknown. A common way to avoid this difficulty is to regularize (4.2), see e.g. [4, 27]. Following [4], instead of (4.2) we set

$$\boldsymbol{\tau} = 2\mu\mathbf{D}\mathbf{u} + \tau_s \frac{\mathbf{D}\mathbf{u}}{\sqrt{\varepsilon^2 + |\mathbf{D}\mathbf{u}|^2}} \tag{4.3}$$

for some small $\varepsilon > 0$. This enables us to consider the system of equations (4.1) and relations (4.3) in the whole computational domain and brings us to the model problem (1.2) with

$$\nu(\mathbf{x}) = 2\mu + \frac{\tau_s}{\sqrt{\varepsilon^2 + |\mathbf{D}\mathbf{u}(\mathbf{x})|^2}}.$$

From modeling reasons the parameter ε should be small enough to ensure that the non-Newtonian fluid described by (4.1) and (4.3) well approximates the viscoplastic medium. The well-known result [14] is

$$\|\nabla(\mathbf{u} - \mathbf{u}_\varepsilon)\| \leq c\sqrt{\varepsilon}, \tag{4.4}$$

where $\mathbf{u}$ and $\mathbf{u}_\varepsilon$ are the solutions to the non-regularized (4.1), (4.2) and regularized (4.1), (4.3) problems, respectively.We will see that reasonably small (from the modeling point of view) values of ε may lead to the serious loss of efficiency of linear and non-linear iterative solvers. If we assume $\mathbf{u} \in W^1_\infty(\Omega)$, $\mu = O(1)$, and $\tau_s > 0$, then for the spectrum bounds in (3.1) we have $c_0^2 \nu_{\max}^{-1} = O(\varepsilon)$, $\nu_{\min}^{-1} = O(1)$. This leads to the following estimate of the condition number

$$\operatorname{cond}(M^{-1}S) \leq c\,\frac{1}{\varepsilon}. \tag{4.5}$$

Indeed, numerical experiments of section 5 show that the bound (4.5) is sharp with respect to ε and the convergence of a Krylov subspace solver with block preconditioner (2.4) and $\widehat{S} = M$ seriously deteriorates for small ε. Same experiments show that the

preconditioning with M_ν leads to a significantly better convergence. To explain this numerical observation we consider an analytical solution to the Bingham problem and evaluate the constant $\tilde{c}_\nu$ given by lemma 3.4.

Unlike the Stoke case, not a lot of reasonable analytical solutions are known for the Bingham problem. One is the flow between two planes: $\mathbf{u} = (u, v, w)$ with

$$\begin{aligned} u &= \begin{cases} \frac{1}{8}(1-2\tau_s)^2, & \text{if } \frac{1}{2}-\tau_s \le y \le \frac{1}{2}+\tau_s, \\ \frac{1}{8}\left[(1-2\tau_s)^2 - (1-2\tau_s-2y)^2\right], & \text{if } 0 \le y < \frac{1}{2}-\tau_s, \\ \frac{1}{8}\left[(1-2\tau_s)^2 - (2y-2\tau_s-1)^2\right], & \text{if } 1 \ge y > \frac{1}{2}+\tau_s, \end{cases} \\ v &= w = 0, \\ p &= -x. \end{aligned} \tag{4.6}$$

The rigid region consists of a constantly moving kernel for $\frac{1}{2}-\tau_s \le y \le \frac{1}{2}+\tau_s$. The yield stress $\tau_s = 0.5$ is the critical value, when the flow region disappears. The solution can be considered in the 3D as well as in the 2D case.

Let $\Omega = (0,1)^d$. To apply lemma 3.4 we set Ω_1 equal to the rigid zone; Ω_2 and Ω_3 are two flow regions given by $0 < y < \frac{1}{2}-\tau_s$ and $1 > y > \frac{1}{2}+\tau_s$, respectively. Since $\nu = const > 0$ in Ω_1 we get $\nabla \nu^{-\frac{1}{2}} = 0$ in Ω_1 and $\tilde{c}_\nu(\Omega_1) = O(1)$. In Ω_2 one finds by the straightforward computations $\|\nabla \nu^{-\frac{1}{2}}\|_{L^\infty(\Omega_2)} = O(1)$ and $\|\nu^{\frac{1}{2}}\|_{L^k(\Omega_2)} = O(\varepsilon^{\frac{2-k}{2k}})$ for $k > 2$. The same relations hold for Ω_3. Therefore we get for the constant $\tilde{c}_\nu(\Omega)$ given by lemma 3.4: $\tilde{c}_\nu(\Omega) \ge c(s)\varepsilon^{-s}$ for any $s > 0$ in the 2D case and $\tilde{c}_\nu(\Omega) \ge c\,\varepsilon^{-\frac{1}{3}}$ in the 3D case. If we assume that similar estimates are enjoyed by the constant from the discrete counterpart of (3.11), than due to (3.27) we get

$$\begin{aligned} d = 2: &\qquad \lambda_{\max}(M_\nu^{-1}S)/\lambda_7(M_\nu^{-1}S) \le c(s)\,\varepsilon^{-s} \qquad \forall\ s > 0 \\ d = 3: &\qquad \lambda_{\max}(M_\nu^{-1}S)/\lambda_7(M_\nu^{-1}S) \le c\,\varepsilon^{-\frac{1}{3}} \end{aligned} \tag{4.7}$$

Comparing to (4.5) we see that the the simple preconditioning with M_ν ameliorates much of the bad scaling of the condition number with respect to ε. The influence of λ_n, $n = 2, \dots, 6$ on the convergence of a Krylov subspace method would be neutralized by at most 5 additional iterations.

Finally, we note that regularized models different from (4.3), e.g. from [27], can be considered in the same way.

5. Numerical results. In this section we give results of several numerical experiments for the equations of the regularized Bingham model. The goal of these experiments is to test the preconditioners discussed in section 2 and to verify whether the analysis from sections 3 and 4 is predictive. To run the numerical experiments we use two different discretizations. One is given by the finite element method (2.2) with isoP2-P1 elements for the velocity-pressure spaces $\mathbb{V}_h$–$\mathbb{Q}_h$. This pair of spaces satisfies the LBB condition (2.1). Another one is the extension of the well-known MAC finite-difference scheme ([13]) for the case of non-Newtonian flows as described in [21]. Both discretizations use the uniform grid with mesh-size h.

5.1. Linearized problem. First we consider in $\Omega = (0,1)^2$ the linearized problem (1.6) with

$$\nu(\mathbf{x}) = \nu(|\mathbf{D}\mathbf{u}(\mathbf{x})|) = 2\mu + \frac{\tau_s}{\sqrt{\varepsilon^2 + |\mathbf{D}\mathbf{u}(\mathbf{x})|^2}}$$

TABLE 5.1
Eigenvalues of $M^{-1}S$ and $M_\nu^{-1}S$: FD with $h = \frac{1}{32}$ and FE with $h = \frac{1}{16}$; $\tau_s = 0.3$

ε	$\lambda_2(M^{-1}S)$	$\lambda_{\max}(M^{-1}S)$	$\lambda_2(M_\nu^{-1}S)$	$\lambda_3(M_\nu^{-1}S)$	$\lambda_{\max}(M_\nu^{-1}S)$
	MAC				
0.1	3.258e-1	0.284	3.428e-1	3.465e-1	1.042
0.01	7.982e-2	0.265	1.129e-1	1.129e-1	1.460
1e–3	8.705e-3	0.264	2.969e-2	3.457e-2	1.873
1e–4	8.783e-4	0.264	3.240e-3	2.526e-2	1.983
1e–5	8.791e-5	0.264	3.271e-4	2.427e-2	1.998
	isoP2-P1				
0.1	3.027e-2	0.233	1.116e-1	1.160e-1	1.010
0.01	1.385e-2	0.189	1.101e-1	1.109e-1	1.362
1e–3	1.470e-3	0.185	6.164e-2	6.208e-2	1.707
1e–4	1.480e-4	0.185	7.543e-3	4.456e-2	1.687
1e–5	1.481e-5	0.184	7.725e-4	4.260e-2	1.494

where the velocity vector field $\mathbf{u}$ is known and given by (4.6). We fix $\mu = 1$, $\tau_s = 0.3$ and vary regularization parameter ε and mesh size. Both finite difference (FD) and finite element (FE) discretizations lead to the saddle-point type system (2.3). For the FE method, matrix M is the pressure mass matrix and M_ν is defined in (3.8). For finite differences, the corresponding choices are $M = I$ (I is the identity matrix) and $M_\nu = diag(\nu^{-1}(\mathbf{x}_i))$, i.e. the i-th main-diagonal element is equal to $\nu^{-1}(\mathbf{x}_i)$, where $\mathbf{x}_i$ denotes the grid node corresponding to the i-th pressure degree of freedom.

Table 5.1 shows few minimal nonzero and maximal eigenvalues for $M^{-1}S$ and $M_\nu^{-1}S$ (recall that $\lambda_1 = 0$ in both cases). Figure 5.1 plots all eigenvalues for $\varepsilon = 10^{-3}$ and $\varepsilon = 10^{-5}$ and FD discretization. For the FE discretization the eigenvalues plots are not shown, since they are qualitatively similar to the FD case. We observe the asymptotic

$$\begin{aligned} &\lambda_2(M^{-1}S) = O(\varepsilon), \quad \lambda_{\max}(M^{-1}S) = O(1) \qquad \text{and} \\ &\lambda_2(M_\nu^{-1}S) = O(\varepsilon), \quad \lambda_{\max}(M_\nu^{-1}S) = O(1). \end{aligned} \tag{5.1}$$

For other eigenvalues it clearly holds

$$\lambda_k(M^{-1}S) = O(\varepsilon) \quad \text{for} \quad k = 3, \dots K, \quad \text{with} \quad K \gg 1, \tag{5.2}$$

but

$$\lambda_k(M_\nu^{-1}S) = O(1) \quad \text{for} \quad k \geq 3. \tag{5.3}$$

Results in (5.1)–(5.3) agree very well with the theoretical eigenvalue bounds in (4.5) and (4.7) and the upper bounds given by lemmas 3.1 and 3.2, suggesting that these bounds are almost sharp in terms of ε. In particular, the ε-dependence of the minimal nonzero eigenvalue of $M_\nu^{-1}S$ indicates that the lack of an estimate for the few smallest eigenvalues in (3.27) is not an artifact of the proof. Thus, for the present example our analysis predicts almost ε-independent bound for λ_7, while experiments show that such a bound is likely to hold already for λ_3. From figure 5.1 we see that the ν-dependent preconditioner M_ν leads to a better clustering of the eigenvalues. This property will be even more evident for the non-analytical example in § 5.2.2 (fig. 5.3).

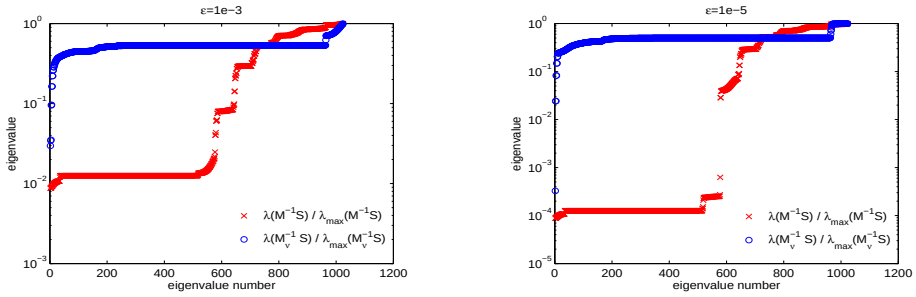

FIG. 5.1. *All nonzero eigenvalues for* $\varepsilon = 10^{-3}$ *(left) and* $\varepsilon = 10^{-5}$ *(right) for* $h = \frac{1}{32}$ *and* $\tau_s = 0.3$

TABLE 5.2
Eigenvalues of $\widehat{M}_\nu^{-1} M_\nu$ *for FE method with* $h = \frac{1}{16}$ *and* $\tau_s = 0.3$.

ε	0.1	0.01	1e–3	1e–4	1e–5
$\lambda_1(\widehat{M}_\nu^{-1} M_\nu)$	0.500	0.499	0.498	0.498	0.497
$\lambda_{\max}(\widehat{M}_\nu^{-1} M_\nu)$	2.000	2.002	2.004	2.004	2.005

For finite element discretizations one is also interested in having a simple approximation for the mass type matrix M_ν, since M_ν^{-1} is not a sparse matrix in contrast to the finite difference case. The table 5.2 shows that the diagonal matrix $\widehat{M}_\nu = diag(M_\nu)$ is a very good approximation to M_ν. Thus for finite element problem one can set $\widehat{S} = \widehat{M}_\nu$, or define $\widehat{S}^{-1} z$ through a fix number of linear iterations for solving the system $\widehat{M}_\nu^{-1} M_\nu y = \widehat{M}_\nu^{-1} z$ with the zero initial guess.

5.2. The Bingham problem. Further we solve numerically the nonlinear problem (4.1), (4.3) with Picard iterations (1.2). We will monitor the convergence of the linear and nonlinear solvers as well as solution accuracy for different values of ε.

5.2.1. Analytical test. Below we consider the regularized Bingham problem in a channel. For this problem we know the exact solution in the limit case of $\varepsilon = 0$, i.e. $\mathbf{u}$ given by (4.6). On every iteration of (1.2) the linearized problem (1.5) was solved by MINRES iterative method with preconditioner (2.4). For $\widehat{A}$ we take the exact factorization for the (1,1)-submatrix A, the choice of $\widehat{S}$ was described in § 5.1. The accuracy is measured in the discrete L^2 norm for velocity and pressure:

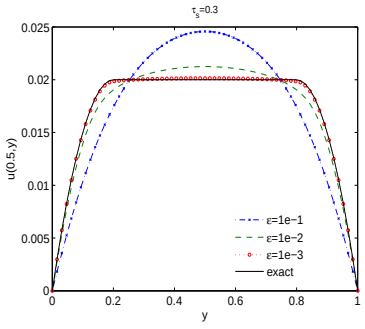

FIG. 5.2. *Velocity profiles of discrete solutions for different* ε.

$$err_u = \frac{\|\mathbf{u} - \mathbf{u}_h\|}{\|\mathbf{u}\|}, \quad err_p = \frac{\|p - p_h\|_{L^2(\Omega_f)}}{\|p\|_{L^2(\Omega_f)}},$$

where Ω_f is the flow region, $\Omega_f = \Omega_2 \cap \Omega_3$. Table 5.3 shows the discrete solution accuracy for different values of ε, the total number of Picard iterations and the average number of the inner MINRES iterations. To calculate results from table 5.3 we stop the outer Picard iterations when the ℓ_2-norm of the nonlinear residual was less than 10^{-4} and the inner MINRES iterations were stopped once the ℓ_2-norm of the initial residual has been reduced by at least five

orders of magnitude. We note that setting such a tight inner tolerance is often not necessary in practice. The linearized problem on every non-linear iteration can be solved with a lower accuracy. We will illustrate this option for the driven cavity test problem in the next section.
In agreement with our analysis the choice of $\widehat{S} = M_\nu$ makes the performance of the linear iterations robust with respect to the parameter ε, while for the simple choice $\widehat{S} = M$ the number of inner iterations increases for $\varepsilon \to 0$. For the present example and the value of h it does not make sense to decrease ε below 10^{-4} or 10^{-5}, since the discretization error begins to dominate over modeling error. The velocity profiles of $u_h(\frac{1}{2}, y)$ are shown on figure 5.2 (with $h = \frac{1}{32}$, $\tau_s = 0.3$ and varying ε).

TABLE 5.3
Solution accuracy and iteration numbers for channel flow with $\tau_s = 0.3$, $h = \frac{1}{32}$ for MAC discretization; Inner iterations tolerance: 10^{-5}.

	ε				
	0.1	0.01	1e–3	1e–4	1e–5
err_u	1.38e-1	3.77e-2	5.73e-3	1.53e-3	1.34e-3
err_p	3.79e-1	1.33e-1	4.48e-2	2.30e-2	2.03e-2
#Picard iter.	10	24	51	61	81
#linear iter. $\widehat{S} = M$	13.8	27.0	56.7	92.3	147
#linear iter. $\widehat{S} = M_\nu$	13.7	19.8	25.8	26.5	25.9

5.2.2. Driven cavity test. The next test is the two-dimensional lid-driven cavity problem: $\Omega = (0,1)^2$, $\mathbf{f} = 0$, with $\mathbf{u}(\mathbf{x})|_{y=1} = (1,0)$ and homogeneous Dirichlet boundary conditions on the rest part of the boundary. The solution has a non-physical singular behavior in the upper corners; however the problem serves as a standard benchmark for incompressible CFD codes.

TABLE 5.4
Iteration numbers for driven cavity problem $h = \frac{1}{32}$. Inner iterations tolerance: 10^{-2}.

	MAC				isoP2-P1			
ε	0.1	0.01	1e–3	1e–4	0.1	0.01	1e–3	1e–4
	$\tau_s = 2$				$\tau_s = 2$			
#Picard iter.	22	63	103	119	23	77	214	430
#linear iter. $\widehat{S} = M$	8.8	12.3	22.8	46.1	4.9	7.6	10	30[1]
#linear iter. $\widehat{S} = M_\nu$	7.5	6.6	5.9	6.0	3.0	2.4	2.1	2.4
	$\tau_s = 5$				$\tau_s = 5$			
#Picard iter.	34	81	117	127	37	118	287	454
#linear iter. $\widehat{S} = M$	9.4	15.2	28.8	54.4	5.4	8.3	11.6	35[1]
#linear iter. $\widehat{S} = M_\nu$	7.4	7.2	6.6	6.4	2.3	2.3	2.3	2.1

Table 5.4 shows the total number of Picard iterations and the average number of inner MINRES (or BiCGstab for isoP2-P1) iterations for different values of ε. To

[1] In these runs the inner stopping criteria was tighten to 10^{-3}. Otherwise the outer iterations (1.2) do not converge.

TABLE 5.5
Eigenvalues of $M^{-1}S$ and $M_\nu^{-1}S$ on the last Picard iteration for the driven cavity problem; isoP2-P1 with $h = \frac{1}{16}$.

	$\tau_s = 2$				$\tau_s = 5$			
ε	0.1	0.01	1e–3	1e–4	0.1	0.01	1e–3	1e–4
$\lambda_2(M^{-1}S)$	5.45e-3	5.96e-4	6.02e-5	6.03e-6	2.30e-3	2.39e-4	2.34e-5	2.40e-6
$\lambda_{\max}(M^{-1}S)$	0.377	0.376	0.376	0.376	0.307	0.306	0.306	0.306
$\lambda_2(M_\nu^{-1}S)$	1.13e-1	1.12e-1	1.12e-1	1.12e-1	1.02e-1	9.83e-2	9.30e-2	9.14e-2
$\lambda_{\max}(M_\nu^{-1}S)$	1.435	1.678	1.626	1.358	1.566	1.790	1.749	1.688

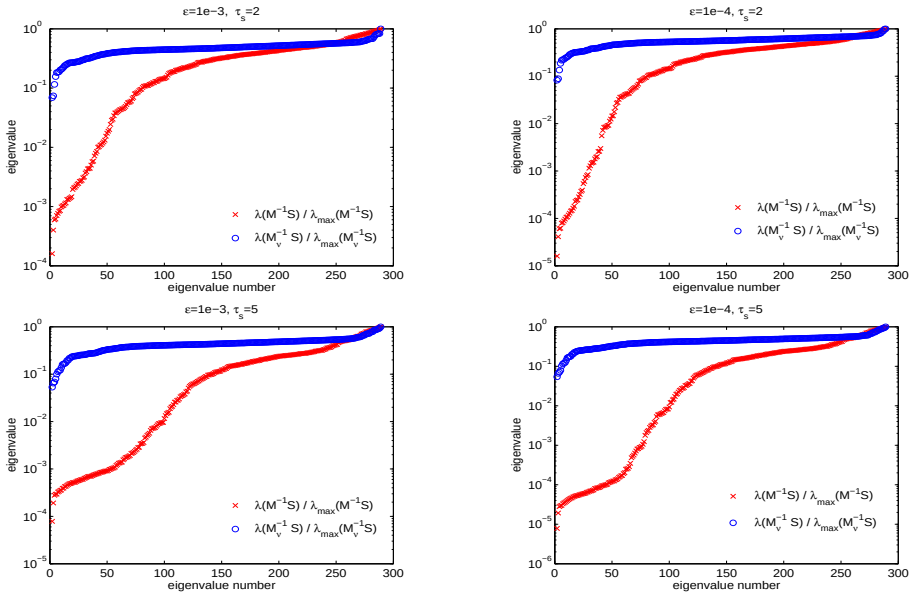

FIG. 5.3. *All (scaled) nonzero eigenvalues on the last Picard iteration for the driven cavity problem with $\tau = 2$ (upper) and $\tau = 5$ (bottom), $\varepsilon = 10^{-3}$ (left) and $\varepsilon = 10^{-4}$ (right); isoP2-P1 with $h = \frac{1}{16}$*

produce results from table 5.4 we take the solution of the Stokes problem ($\tau_s = 0$) as the initial guess and stop the outer Picard iterations, when the ℓ_2-norm of nonlinear residual was reduced by at least the factor 10^5. Unlike the previous test, the tolerance for the inner iterations was taken less tight, i.e. the inner MINRES iterations were stopped once the ℓ_2-norm of the initial residual has been reduced by 10^2. Such weakening of the inner tolerance has almost no affect on the total number of the outer iterations; similar observation can be found, e.g. in [17]. Similar to the analytical test, the choice of $\widehat{S} = M_\nu$ makes the performance of the linear iterations robust with respect to the parameter ε, while for the simple choice $\widehat{S} = M$ the number of inner iterations increases for $\varepsilon \to 0$. We recall that for the finite element discretization we use the BiCGstab inner solver with triangular preconditioner (2.5). One iteration of BiCGstab is approximately twice as expensive as one iteration of MINRES.

Further we look for the eigenvalues distribution of $M^{-1}S$ and $M_\nu^{-1}S$. Thus,

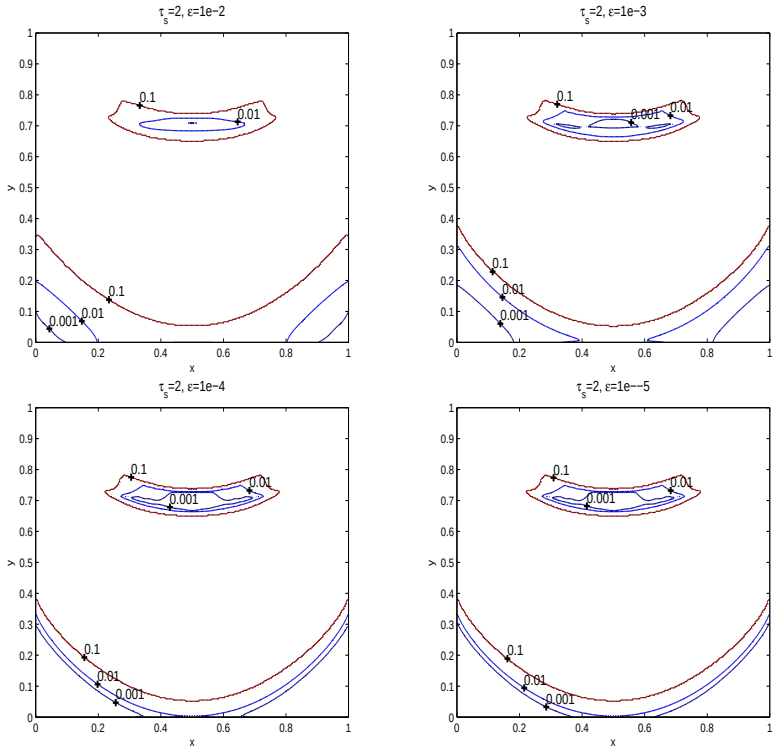

FIG. 5.4. *Approximation of the rigid zones for the driven cavity problem with* $\tau_s = 2$ *and varying* ε*: isolines for* $|\mathbf{D}\mathbf{u}_h|$ *with values* $= \{10^{-1}, 10^{-2}, 10^{-3}\}$

table 5.5 shows minimal nonzero and maximal eigenvalues for $M^{-1}S$ and $M_\nu^{-1}S$ ($\lambda_1 = 0$ in both cases) and figure 5.1 plots all eigenvalues for $\varepsilon = 10^{-3}$ and $\varepsilon = 10^{-4}$ and two values of the stress yield τ_s. Again we observe that $\lambda_2(M^{-1}S) = O(\varepsilon)$ and $\lambda_{\max}(M^{-1}S) = O(1)$. With the new preconditioner both the second and the maximal eigenvalues of $M_\nu^{-1}S$ are uniformly bounded with respect to ε. We note that for small ε the number of outer nonlinear iterations significantly increases. To improve the situation one might consider Newton type methods instead of the Picard iterations. This would lead to a more complicated linear algebraic system to be solved on each non-linear iteration. Moreover, results in [17, 8] show that the Newton approach is not robust with respect to ε as well.

From the modeling point of view the most challenging task is finding the rigid regions of the viscoplastic fluid flow. Formally, these are the regions, where $\mathbf{D}\mathbf{u}_h = 0$. The latter condition, however, does not hold exactly for the numerical solution, especially if a regularized model is used. For the driven cavity problem some numerical results, including the prediction of the rigid zones can be found in [9, 11, 20, 23, 36]. In [20, 11] a regularized model has been used, while [9, 23, 36] considered the non-regularized Bingham model. To give an insight into the quality of the discrete solution for different values of the regularization parameter ε, the figures 5.4 and 5.5 show computed isolines of $|\mathbf{D}\mathbf{u}_h|$ for $\varepsilon \in \{10^{-2}, 10^{-3}, 10^{-4}, 10^{-5}\}$. We plot the isolines with the values $\{10^{-1}, 10^{-2}, 10^{-3}\}$. From these results and the results of the papers cited above it follows that for $\varepsilon \lesssim 10^{-4}$ the region where $|\mathbf{D}\mathbf{u}_h| \lesssim 10^{-3}$ gives a fairly good prediction of a rigid zone. At the same time, the values of the regularization

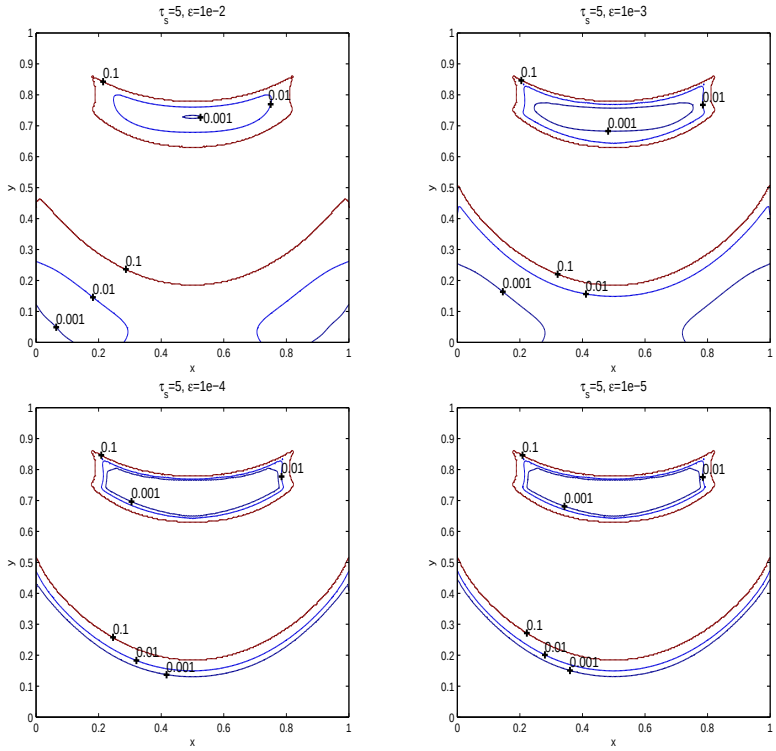

FIG. 5.5. *Approximation of the rigid zones for the driven cavity problem with* $\tau_s = 5$ *and varying* ε*: isolines for* $|\mathbf{D}\mathbf{u}_h|$ *with values* $= \{10^{-1}, 10^{-2}, 10^{-3}\}$

parameter $\varepsilon \gtrsim 10^{-3}$ are not small enough to recover the viscoplastic behavior of fluid. Note that the sufficiently small (from the modeling point of view) values of ε are those values when the developed preconditioner M_ν gives significant improvement of the linear solver performance.

REFERENCES

[1] Bank, R., Welfert, B.D., Yserentant, H., A class of iterative methods for solving saddle point problems, Numer. Math., V. 56 (1990), 645-666.
[2] Brezzi, F., Fortin, M. Mixed and hybrid finite element methods, New-York: Springer, 1991.
[3] Benzi M., Golub G.H., Liesen J., Numerical solution of saddle point problems, Acta Numerica, V.14 (2005), 1–137.
[4] Bercovier M., Engelman M., A finite element method for incompressible non-newtonian flows, J.Comp.Phys. V.36 (1980), 313–326.
[5] Bramble J., Pasciak J., A preconditioning technique for indefinite systems resulting from mixed approximation of elliptic problems, Math. Comp., V.50 (1988), 1–17.
[6] Cahouet J., Chabard J.P., Some fast 3D finite element solvers for the generalized Stokes problem, *Int. J. Numer. Methods Fluids.*, V. 8 (1988), 869–895.
[7] Christensen U., Harder H., 3-D Convection With Variable Viscosity, Geophysical Journal International, V. 104 (2007), pp. 213–220
[8] Dean E.J., Glowinski R., Operator-splitting methods for the simulation of Bingham visco-plastic flow, Chin. Ann. of Math. V.23 (2002), 187–204.
[9] Dean E. J., Glowinski R., Guidoboni G., On the numerical simulation of Bingham visco-plastic flow: Old and New results, J.Non-Newtonian Fluid Mech. V.142 (2007), 36–62.
[10] Duvaut G., Lions J. L. Inequalities in Mechanics and Physics, Springer, 1976

[11] Elias R. N., Martins M.A.D., Coutinho A.L.G.A., Parallel edge-based solution of viscoplastic flows with the SUPG/PSPG formulation, Comput. Mech. 38 (2006) 365-381
[12] Elman H.C., Silvester D.J., Wathen A.J., Finite Elements and Fast Iterative Solvers: with Applications in Incompressible Fluid Dynamics, Numerical Mathematics and Scientific Computation, Oxford University Press, Oxford, UK, 2005.
[13] Fletcher C.A.J., Computational Techniques for Fluid Dynamics, Springer-Verlag, Sydney, 1990.
[14] Glowinski R., Numerical Methods for Nonlinear Variational Problems, Springer Verlag, New York, NY, 1984.
[15] Hackbusch, W. Multi-grid Methods and Applications, Berlin, Heidelberg: Springer, 1985.
[16] Hron, J., Malék, J., Necãs J., Rajagopal, K. R., Numerical simulations and global existence of solutions of two-dimensional flows of fluids with pressure- and shear-dependent viscosities, Mathematics and Computers in Simulation, V.61 (2003), 297–315.
[17] Hron, J., Ouazzi, A., Turek, S. A Computational Comparison of two FEM Solvers For Nonlinear Incompressible Flow. In Challenges in Scientific Computing. Springer, 2004. Cisc 2002.
[18] Kobelkov G.M., Olshanskii M.A., Effective Preconditioning of Uzawa Type Schemes for Generalized Stokes Problem, Numer. Math., V.86 (2000), 443–470
[19] Malék, J., Necãs, J., Rajagopal, K. R., Global Existence of Solutions for Flows of Fluids with Pressure and Shear Dependent Viscosities, Applied Mathematics Letters, V.15 (2002), 961–967.
[20] Mitsoulis E., Zisis Th., Flow of Bingham plastics in a lid-driven cavity. J. Non-Newtonian Fluid Mech. 101 (2001), 173–180.
[21] Muravleva E.A., Olshanskii M.A., Two finite-difference schemes for the Bingham cavity flows, Rus. J. Num. Anal. Math. Model. V.23 (2008), 615–634
[22] Olshanskii M.A., Lections and exercises in multigrid methods, Fizmatlit, Moscow 2005
[23] Olshanskii M.A., Analysis of semi-staggered finite-difference method with application to Bingham flows, *Comp. Meth. Appl. Mech. Eng.* (2008), doi:10.1016/j.cma.2008.11.010
[24] Olshanskii M.A., Reusken A., Analysis of a Stokes interface problem, Numerische Mathematik, V. 103 (2006), 129–149.
[25] Olshanskii M.A., Vassilevski Yu.V., Pressure Schur complement preconditioners for the discrete Oseen problem, SIAM J.Sci.Comp. V. 29 (2007) 2686–2704.
[26] Ouazzi A., Turek S., Hron J., Finite element methods for the simulation of incompressible powder flow, Comm. Num. Meth. Engr. V. 21 (2005) 581–596.
[27] Papanastasiou T.C., Flows of materials with yield, J.Rheol. V.31 (1987) 385–404.
[28] Quarteroni A., Valli A., Domain Decomposition Methods for Partial Differential Equations, Oxford University Press, 1999
[29] Saad, Y., Iterative methods for sparse linear systems, New-York: ITP, 1996.
[30] Schaeffer, D. G., Instability in the evolution equation describing incompressible granular flow, J. of Differential Equations, V.66 (1987), 19–50.
[31] Silvester D., Wathen A., Fast Iterative Solution of Stabilised Stokes Systems, Part II: Using General Block Preconditioners, SIAM J. Num. Anal., V.31 (1994), 1352–1367.
[32] Ruge J. W., Stüben K., Algebraic multigrid. Multigrid Methods, edited by S. McCormick, 1987
[33] Tackley P.J., Effects of strongly variable viscosity on three-dimensional compressible convection in planetary mantles, J. Geophys. Res., V. 101 (1996), 3311–3332.
[34] Temam R., Navier-Stokes Equations: Theory and Numerical Analysis, North-Holland, New-York, 1979
[35] Tennekes H., Lumley J.L., A First Course in Turbulence, MIT Press, 1972
[36] Vola D., Boscardin L., Latche J.C., Laminar unsteady flows of Bingham fluids: a numerical strategy and some benchmark results, J.Comput. Physics 187 (2003) 441–456.
[37] Wathen A., Realistic eigenvalues bounds for the Galerkin mass matrix, IMA J. Numer. Anal., V.7 (1987), 449–457.